

# Formation energy, lattice relaxation, and electronic structure of Al/Si/GaAs(100) junctions

C. Berthod, N. Binggeli, and A. Baldereschi

*Institut Romand de Recherche Numérique en Physique des Matériaux (IRRMA), CH-1015 Lausanne, Switzerland*

(Received 2 October 1997)

We investigated the energetics as well as the structural and electronic properties of chemically abrupt Al/GaAs(100) and engineered Al/Si/GaAs(100) Schottky diodes with 2 monolayers of Si using the *ab initio* pseudopotential approach. Results for the atomic relaxation at the interface, its influence on the Schottky barrier, and the dependence of the formation energy on the As and Ga chemical potentials are presented. We show that a reversal in the relative stability of the As- and Ga-terminated junctions occurs within the experimentally accessible range of the As and Ga chemical potentials, for both Al/GaAs and Al/Si/GaAs interfaces. This reversal could explain the role played by the excess cation and anion flux in the fabrication of tunable Al/Si/GaAs(100) Schottky diodes. [S0163-1829(98)04716-X]

## I. INTRODUCTION

Tunable Schottky barriers were recently demonstrated in metal/*n*-GaAs(100) junctions engineered with group-IV atomic interface layers.<sup>1-4</sup> The metal/GaAs barrier heights were shown to increase or decrease by as much as 0.4 eV according to whether the interlayers — grown by molecular beam epitaxy — were fabricated under an excess cation (Ga or Al) or anion (As) flux. Although such changes were first observed in junctions containing 10 to 60 Å thick interlayers, Cantile *et al.*<sup>3</sup> demonstrated more recently that the barrier modifications in engineered Al/Si/GaAs(100) systems are already established for Si coverages as low as 2 monolayers (ML).

As the atomic-scale morphologies of these buried interfaces are difficult to probe experimentally, the influence of the different excess fluxes on the interface atomic structure is as yet unknown. We have recently shown,<sup>5</sup> however, based on *ab initio* calculations, that local interface dipoles generated by replacing anion-cation pairs by Si pairs at As- and Ga-terminated GaAs(100) interfaces could quantitatively explain the Al/Si/GaAs(100) Schottky barrier tuning observed experimentally in the range 0–2 Si ML.<sup>3</sup> In this article, we address the relative stability of the As- and Ga-terminated Al/Si/GaAs(100) junctions, and the role the excess fluxes may play in the formation of these interfaces.

The growth process per se involves complex kinetic mechanisms whose description is far beyond the scope of the present study. Here we will concentrate on the energetics of the Ga- and As-terminated interfaces, and show that the experimental trend can already be accounted for based on a thermodynamic description. In this study, we will consider abrupt Al/Si/GaAs(100) junctions, and focus on the limiting cases of Si coverages  $\theta=0$  and 2 ML. Using these prototype systems, we will examine the atomic relaxation, the formation energy and the electronic structure of the As- and Ga-terminated junctions, and discuss their relative stability under different experimental conditions.

## II. METHOD

Our calculations were carried out within the local-density functional (LDF) framework, using the pseudopotential

method.<sup>6</sup> We employed norm-conserving Troullier-Martins pseudopotentials in the Kleinman-Bylander nonlocal form<sup>7</sup> and the exchange-correlation functional of Ceperley and Alder.<sup>8</sup> The electronic states were expanded on a plane-wave basis set using a kinetic energy cutoff of 20 Ry.<sup>9</sup> We modeled the As- (Ga-) terminated Al/GaAs(100) junctions with supercells containing 13 Al layers, and 7 As (Ga) plus 6 Ga (As) layers. The Al [100] axis was made parallel to the GaAs [100] growth direction, and the Al fcc lattice was rotated 45° about the [100] axis relative to the semiconductor in order to satisfy epitaxial conditions.<sup>10</sup> The Ga-As bilayer nearest to the metal was then replaced by Si to generate the initial Al/Si/GaAs junctions with As-terminated (hereafter denoted as type I) and Ga-terminated (type II) interfaces. In these heterostructures, the Al overlayer can be viewed as a superposition of two sublattices. In one of the sublattices the Al (Al<sup>(S)</sup>) occupy substitutional sites in the continuation of the bulk semiconductor structure, whereas in the other sublattice the Al (Al<sup>(I)</sup>) occupy interstitial (octahedral) sites of the zinc-blende structure (see Fig. 1).

The supercell calculations were performed with a (2, 6, 6) Monkhorst-Pack *k*-point grid.<sup>11</sup> The theoretical lattice parameter of GaAs  $a^{\text{GaAs}}=5.55$  Å ( $a^{\text{GaAs}}(\text{exp})=5.65$  Å), was used. The interface geometries that we will refer to as unrelaxed in the following (also used in Ref. 5 to study the Schottky barriers) were constructed using macroscopic elasticity theory (MET) to determine the deformation of the Al

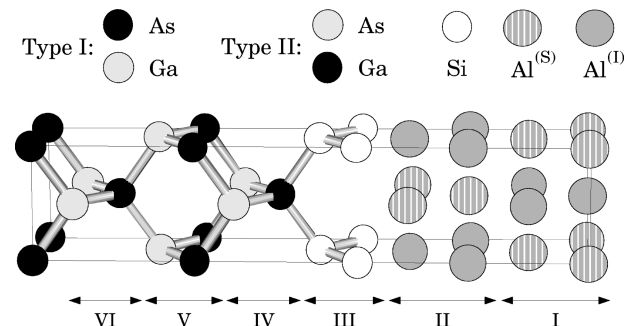


FIG. 1. Epitaxial geometry for the Al/2 Si ML/GaAs(100) junctions with the As-terminated (type I) and Ga-terminated (type II) GaAs(100) interfaces.

overlayer, and neglecting further atomic-scale relaxations taking place at the interfaces. The Al slab in the resulting supercells was tetragonally elongated along the growth direction ( $a_{\perp}^{\text{Al}} = 4.12 \text{ \AA}$ ), and the metal-semiconductor interlayer spacing at the junction was taken as the average between the (100) interlayer spacings in the GaAs and Al bulk parts.

To determine the atomic relaxations at the interfaces, we first considered metal/semiconductor structures with a thin metal overlayer in contact with vacuum. Specifically, our starting configurations for the relaxation runs were generated by removing five atomic layers from the middle of the Al slab in the supercells of the unrelaxed metal/semiconductor structures. The atomic configurations were then fully relaxed, by incorporating the Hellmann-Feynman forces in a gradient procedure to minimize the total energy with respect to the ionic positions. Due to the presence of the vacuum, the metallic overlayer and the interlayers could freely relax along the growth direction, and release thus any residual stress  $\sigma_{xx}$ . To examine the properties of the fully developed junctions, we transferred then the equilibrium interplanar distances to a new supercell including a full Al slab (13 + 13 superlattice). The interlayer spacings for the additional layers at the center of the Al slab were set to their bulk MET value. We then let this structure relax again to allow for small readjustments in the metal. To evaluate the Schottky barrier heights we used the same approach as described in Ref. 5.

### III. LATTICE RELAXATION AND ELECTRONIC STRUCTURE

In Fig. 2 we display the equilibrium interplanar distances as obtained in the Al/GaAs and Al/2 Si ML/GaAs junctions with the thin metallic overlayer (four Al layers), and in the corresponding fully developed junctions (13+13 supercell). As there are two inequivalent Al sublayers in each Al(100) plane, exhibiting some buckling near the interface, we reported in Fig. 2 the largest and the smallest distances between the sublayers in adjacent planes, on the metal side of the junction.

For all of the systems examined here, the distance obtained from the *ab initio* calculation for the separation between the Al surface layer and the central layer of the GaAs slab is identical, within  $0.05 \text{ \AA}$ , to the MET prediction. This is somewhat unexpected given the large relaxations occurring near the junction (more than 10% of the initial spacing in some cases), and the different nature of the materials forming the junction. Except for small readjustments on the Al side of the junction, the relaxations are very similar in the systems with the thin Al overlayer and in the corresponding 13+13 superlattices. The relaxations obtained for the superlattices without the Si interlayer are also consistent with the results by Dandrea and Duke<sup>10</sup> for the Al/GaAs(100) junctions.

Figure 2 shows that the bulk GaAs spacing is recovered beyond the second (Al/GaAs) to third (Al/Si/GaAs) semiconductor layer from the junction, whereas in the metal the bulk (strained) interlayer spacing is recovered only beyond the fourth Al plane from the junction. The relaxations taking place in the metal are qualitatively similar in the four types of metal/semiconductor structures shown in Fig. 2. The

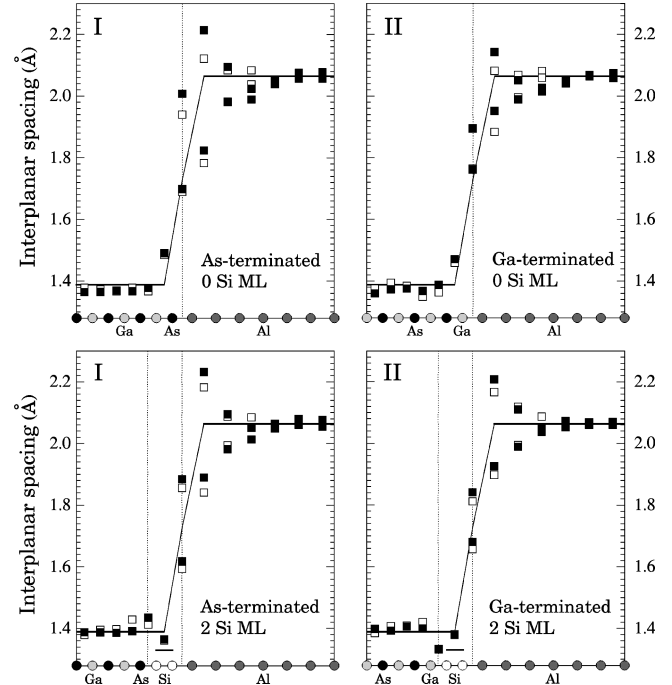


FIG. 2. Equilibrium interplanar spacings for the chemically abrupt As-terminated (left) and Ga-terminated (right) Al/GaAs(100) and Al/2 Si ML/GaAs(100) junctions. Open squares correspond to the system with a thin Al overlayer in contact with vacuum, and solid squares correspond to the 13+13 superlattice (see text). The sequence of atomic layers is indicated at the bottom of each graph. Each Al(100) plane contains two inequivalent sublayers; the largest and smallest distances between sublayers in adjacent planes have been reported on the metal side of the junction. The solid lines show the bulk interplanar spacings. The value of the Si-Si interlayer distance, as obtained from macroscopic elasticity theory for Si pseudomorphically strained to GaAs, is also indicated (short line).

buckling of the first Al layer at the junction reflects the establishment of two types of interfacial bonds: a predominantly covalent (short) type of bonds between the Al<sup>(S)</sup> and the atoms of the semiconductor surface layer, and a metallic (long) type of bonds of the Al<sup>(I)</sup> to the semiconductor. These two types of bonds can be distinguished in the charge density plots presented in Fig. 3 for the type-I and -II Al/Si/GaAs junctions. The Al<sup>(I)</sup> metallic type of bonds across the interface involve predominantly atoms belonging to the first two semiconductor layers (see Fig. 3). The covalent character of the Al<sup>(S)</sup> bond is clearly stronger in the case of the type-I (anion-terminated) relative to the type-II junctions, as reflected by the larger bonding charge density (Fig. 3) and the shorter bond length (Fig. 2) established in this case. Similar covalent and metalliclike charge density features were also observed at the Al/GaAs(100) junctions in Ref. 10.

Without the Si interlayer the As (Ga) surface plane in the type-I (-II) junction moves outwards by about  $0.10 \text{ \AA}$  ( $0.08 \text{ \AA}$ ) relative to the bulk GaAs. There is thus a non-negligible weakening of the covalent bonding between the first two GaAs atomic layers due to the formation of the metallic bonds across the interface. When the Si interlayers are present, the Si-As spacing increases by 3.5% in the type-I junction, whereas the Si-Ga spacing decreases by 4% in the type-II junction relative to the bulk Ga-As spacing. Given

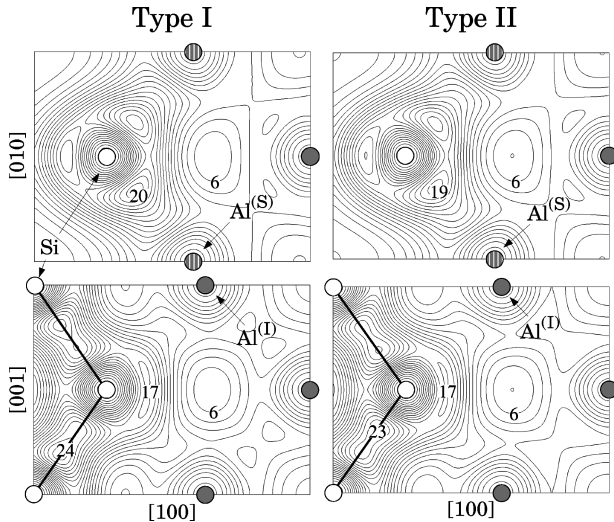


FIG. 3. Contour plots of the Al/2 Si ML/GaAs(100) valence charge density in the (001) and (010) planes (upper and lower panels, respectively) for the type-I (left) and type-II (right) interfaces. The plots show a region including 2 atomic layers of semiconductor and 2 atomic layers of metal. The charge densities are given in units of electrons per bulk GaAs unit cell.

the similar atomic radii of the atomic species involved here, we attribute the increase (decrease) in the Si-As (Si-Ga) interplanar distance to the formation of donor- (acceptor-) type of bonds at the polar Si/GaAs(100) interface. This produces an electronic charge excess (deficit) on the Si-As (Si-Ga) bond, and an elongation (contraction) of the resulting oversaturated (undersaturated) bond.

Closer to the metal, in both types of junctions, the Si-Si interlayer spacing remains, instead, approximately equal (within  $\sim 0.02 \text{ \AA}$ ) to the bulk GaAs interplanar spacing, and is therefore *larger* than the equilibrium spacing in bulk Si ( $a_{\perp}^{\text{Si}} = 101\% a^{\text{Si}}$  for the type-I interface, and  $102\% a^{\text{Si}}$  for the type-II interface). Based on MET, one would have expected the Si-Si interplanar distance to *decrease* with respect to the spacing in bulk Si. In fact, from *ab initio* calculations for bulk Si coherently strained to GaAs we find  $a_{\perp}^{\text{Si}} = 98\% a^{\text{Si}} = 95\% a^{\text{GaAs}}$ . For a two-monolayer-thick Si overlayer grown on GaAs(100), the angle resolved x-ray photoelectron diffraction measurements by Chambers and Loeb's<sup>12</sup> indicate an even larger contraction:  $a_{\perp}^{\text{Si}} = 94\% a^{\text{GaAs}}$ . The reversed trend we find for the Si-Si spacing in the Al/Si/GaAs junctions results from the presence of the metal that weakens the covalent bonding between the two semiconductor layers closest to the Al surface (as also found in the case of the Al/GaAs junctions).<sup>13</sup> We performed similar calculations for a GaAs/2 Si ML/GaAs(100) heterostructure coherently strained to GaAs, and in this case a *contraction* by 5% (7%) of the Si-Si interlayer spacing is obtained with respect to the value in bulk Si (GaAs), consistently with the trend expected from MET and with the results by Chambers and Loeb's for the GaAs/2 Si ML system.

In Fig. 4, we show the local density of states (LDOS) in the relaxed junctions with and without the Si interlayer. The LDOS has been computed in the I–VI supercell regions indicated in Fig. 1. On the semiconductor side of the junction, the LDOS recovers the bulk GaAs density of states features in region VI, i.e., beyond the seventh semiconductor layer

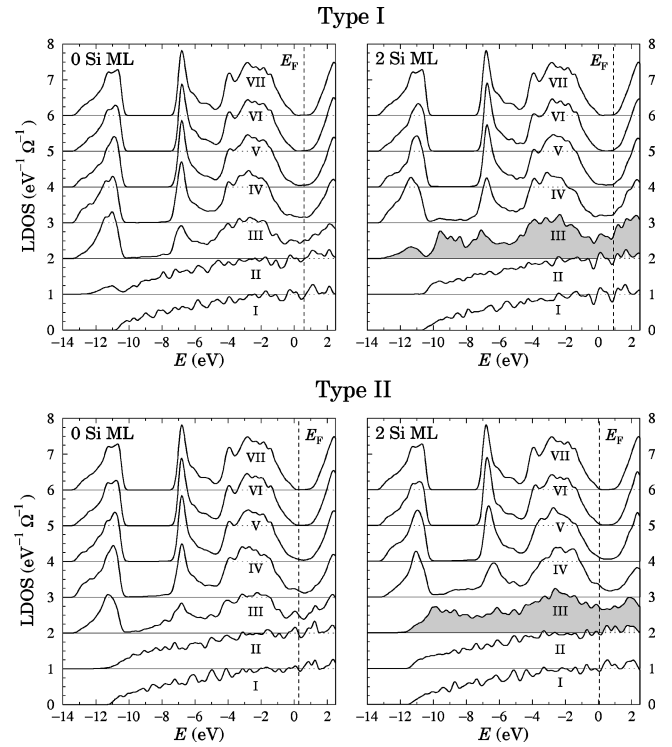


FIG. 4. Local density of states (LDOS) in the Al/GaAs(100) (left) and Al/2 Si ML/GaAs(100) (right) junctions with the type-I and type-II interfaces. The curves correspond to the supercell regions labeled in Fig. 1 (curve VII represents the bulk GaAs density of states). The shaded LDOS correspond to the supercell region including the Si bilayer. The zero of energy has been fixed at the GaAs valence-band edge.  $\Omega$  is the unit-cell volume of bulk GaAs.

from the metal. On the metal side, instead, the bulk Al density of states is essentially recovered beyond the second Al plane from the junction (region I). When the Si bilayer is introduced, the bulk Al LDOS is shifted by  $\approx 0.3 \text{ eV}$  to higher (lower) energies with respect to the bulk GaAs LDOS in the type-I (type-II) junction, as a result of the local interface dipole produced by the heterovalent group-IV atomic substitutions.<sup>5</sup> The calculated values of the Schottky barriers for the different junctions are presented in Table I, both with and without inclusion of lattice relaxation. The Schottky barrier is not affected significantly by the relaxation. In Table I we also show the experimental values of Ref. 3 for the tunable Al/Si/GaAs(100) Schottky barriers. The calculated barriers for the two types of interface termination account very well for the tuning observed experimentally.

The results in Fig. 4 show that the Si interlayer substantially changes the LDOS in the bilayer region III. Without the Si interlayer, the tail of the metal wave functions give rise, in this region, to a finite LDOS of about  $0.5 \text{ eV}^{-1} \Omega^{-1}$  —  $\Omega$  being the bulk GaAs unit-cell volume — for energies in the fundamental bandgap of GaAs. In the presence of the Si bilayer, this LDOS increases to about  $0.7 \text{ eV}^{-1} \Omega^{-1}$  in the GaAs gap region. This large LDOS near the Fermi energy in the engineered junctions is responsible for a large screening of the local interface dipole, and plays an important role in determining the actual barrier modification with the Si bilayer.<sup>5</sup> Figure 4 also shows that the interlayer induces a large density of states in the energy region of the GaAs valence gap. This new LDOS structure, in region III,

TABLE I. Al/Si/GaAs(100) formation energy per surface atom  $\varepsilon_f$  and corresponding  $p$ -type Schottky barrier  $\phi_p$  for the As-terminated (type I) and Ga-terminated (type II) interfaces. Results are reported for Si coverages  $\theta=0$  and 2 monolayers (ML).  $\varepsilon_f$  is evaluated using for the As chemical potential  $\mu_{\text{As}}=\mu_{\text{As}}^{\text{bulk}}$  for the type-I junctions and  $\mu_{\text{As}}=\mu_{\text{As}}^{\text{bulk}}+\Delta H_f$  for the type-II junctions (see text). The LDF values of the Schottky barriers were rigidly shifted by 0.11 eV to take into account many-body and relativistic corrections (Ref. 5). The experimental photoemission data from Ref. 3 are also reported. For the low coverage case, we reported the experimental values measured at 0.2 ML. All energies are in eV.

Interface Type	$\theta$ (ML)	Unrelaxed		Relaxed		Experiment $\phi_p$
		$\varepsilon_f$	$\phi_p$	$\varepsilon_f$	$\phi_p$	
I	0	0.79	0.82	0.58	0.81	0.87–0.89
I	2	0.98	1.14	0.88	1.15	1.15–1.26
II	0	0.80	0.71	0.68	0.61	0.54–0.61
II	2	0.97	0.33	0.90	0.28	0.37–0.46

derives mainly from the  $s$  states of the substitutional Si atoms on the As sites. Due to the weaker ionic potential of Si with respect to that of As, these substitutions push the anion  $s$  states at higher energy relative to the bulk As  $s$ -like feature in GaAs, inducing resonant interface states in the GaAs valence gap.

Our results for the Al/2 Si ML/GaAs LDOS in Fig. 4 and for the Si interlayer relaxation in Fig. 2 call into question the applicability of bulk Si concepts in the explanation of the Al/Si/GaAs Schottky barrier tuning. Recently, Chen *et al.*<sup>14</sup> incorporated the effect of strain in a macroscopic model, based on the properties of degenerate bulk Si, to explain the barrier modifications in terms of band bending and tunneling through the Si interlayer bandgap. The bulk Si bandgap is known<sup>15</sup> to decrease by 40% when Si(100) is coherently strained to the GaAs lattice parameter, as a result of the tetragonal contraction  $\varepsilon_{xx}(\text{Si})\approx-3\%$ . In the model by Chen *et al.*, the Si interlayer contracts according to MET, and has a bandgap of 0.7 eV. Our *ab initio* calculations show, however, that there is no bandgap and no contraction of the Si interlayer in the 0–2 ML coverage regime when the tuning takes place. Our results support, instead, a microscopic process in which Si-induced local interface dipoles change the electrostatic potential-energy lineup, and hence shift the electronic states across the interlayer.

#### IV. FORMATION ENERGY

To discuss the relative stability of the type-I and type-II Al/GaAs(100) and Al/Si/GaAs(100) heterostructures, which contain a different number of Ga and As atoms, it is necessary to compute their formation energy,  $\varepsilon_f$ , as a function of the atomic chemical potentials:

$$\varepsilon_f = F - \sum_i n_i \mu_i \approx E_t - \sum_i n_i \mu_i, \quad (1)$$

where  $n_i$  is the number of atoms and  $\mu_i$  the chemical potential for each atomic species  $i$  in the system.  $F$  is the Gibbs free energy and  $E_t$  the total energy of the system. By definition, the chemical potential  $\mu_i$  is the derivative of the Gibbs

free energy  $F = E_t + PV - TS$  with respect to the number of atoms  $n_i$ . As we are considering here *condensed* matter systems, the pressure term  $PV$  is completely negligible for the pressures we are interested in (i.e., ambient or low pressure), and was discarded in Eq. (1). We also ignored the temperature dependence of the free energy. The temperature-dependent terms tend to cancel out in the free-energy difference between condensed matter phases which yields  $\varepsilon_f$ , and their contribution is expected to be relatively small<sup>16</sup> (of the order or less than  $k_B T$  per surface atom). In this study we will thus use the  $T=0$  values of  $F$  (i.e.,  $E_t$ ) and  $\mu_i$ .

At equilibrium, the Al chemical potential is determined by the total energy per atom of the bulk (strained) Al metal. The As and Ga chemical potentials are related by the condition  $\mu_{\text{As}} + \mu_{\text{Ga}} = \mu_{\text{GaAs}}$  — where  $\mu_{\text{GaAs}}$  is the total energy of bulk GaAs per Ga-As pair — but their difference is, in principle, a free variable. The As (Ga) chemical potential, however, cannot exceed the chemical potential of bulk As (Ga), as bulk As (Ga) would form in the system. Therefore, choosing  $\mu_{\text{As}}$  as independent variable, the range of values of the As chemical potential can be restricted to<sup>16</sup>

$$\mu_{\text{As}}^{\text{bulk}} + \Delta H_f < \mu_{\text{As}} < \mu_{\text{As}}^{\text{bulk}}, \quad (2)$$

where  $\mu_{\text{As}}^{\text{bulk}}$  is the chemical potential of the bulk rhombohedral phase of As,  $\Delta H_f = \mu_{\text{GaAs}} - \mu_{\text{As}}^{\text{bulk}} - \mu_{\text{Ga}}^{\text{bulk}}$  is the heat of formation of GaAs, and  $\mu_{\text{Ga}}^{\text{bulk}}$  is the chemical potential of the bulk orthorhombic phase of Ga. We evaluated the bulk chemical potentials using for the rhombohedral As phase the angle between the unit cell vectors<sup>17</sup>  $\alpha = 54.8^\circ$  and the theoretical equilibrium lattice parameter  $a = 3.70 \text{ \AA}$  [ $a(\text{exp}) = 3.80 \text{ \AA}$ ]. For the Ga orthorhombic structure we used the cell-shape ratios  $b/a = 1.70$ ,  $c/a = 1.00$ ,<sup>17</sup> and the equilibrium lattice parameter  $a = 4.41 \text{ \AA}$  [ $a(\text{exp}) = 4.52 \text{ \AA}$ ]. The Ga internal structural parameters were fully relaxed to determine the equilibrium lattice parameter  $a$  and the corresponding chemical potential. From our calculations,<sup>18</sup> we obtain  $\mu_{\text{As}}^{\text{bulk}} = -173.84 \text{ eV}$ ,  $\mu_{\text{Ga}}^{\text{bulk}} = -61.53 \text{ eV}$ ,  $\mu_{\text{GaAs}} = -236.17 \text{ eV}$ , and hence  $\Delta H_f = -0.80 \text{ eV}$ . Our calculated heat of formation  $\Delta H_f$  compares well with the experimental value of  $-0.85 \text{ eV}$ ,<sup>19</sup> and with earlier *ab initio* calculations.<sup>16</sup> For the formation energies, we expect a similar uncertainty of about 0.1 eV per atom on the absolute values of  $\varepsilon_f$ . As usual, however, within the LDF framework, for relative values we expect a better accuracy of the order of 0.01 eV/atom.

Taking into account that the number of Ga and As atoms differ by one unit in all of our supercells, the formation energies [Eq. (1)] of the type-I and type-II interfaces may be recast as

$$\varepsilon_f^{\text{I}}(\mu_{\text{As}}) = \frac{1}{2}(\mathcal{E}_t^{\text{I}} - \mu_{\text{As}}), \quad (3a)$$

$$\varepsilon_f^{\text{II}}(\mu_{\text{As}}) = \frac{1}{2}(\mathcal{E}_t^{\text{II}} - \mu_{\text{GaAs}} + \mu_{\text{As}}), \quad (3b)$$

where  $\mathcal{E}_t = E_t - n_{\text{GaAs}}\mu_{\text{GaAs}} - n_{\text{Si}}\mu_{\text{Si}} - n_{\text{Al}}\mu_{\text{Al}}$ , and  $n_{\text{GaAs}}$  stands for the number of Ga-As pairs contained in the super-

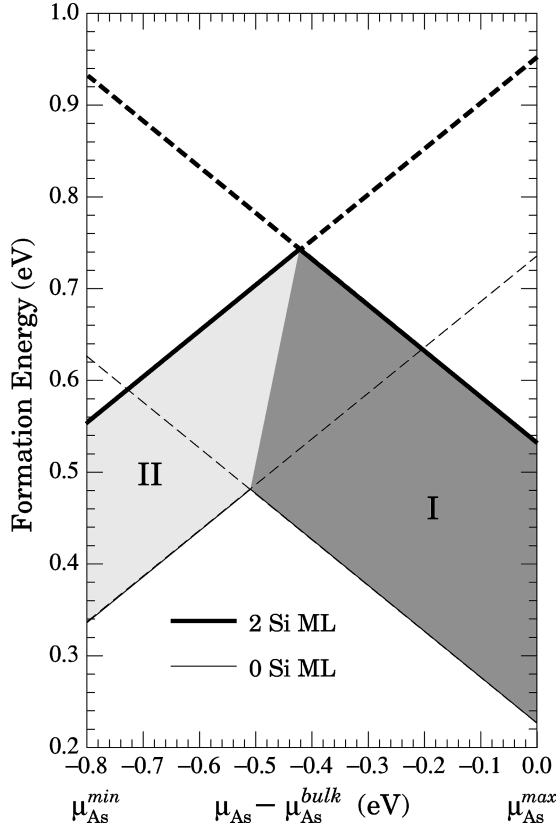


FIG. 5. Al/GaAs(100) and Al/2 Si ML/GaAs(100) formation energies (per semiconductor surface atom) for the type-I and type-II interfaces. The formation energies are displayed in the physically allowed range of values of the As chemical potential (see text).

cell. The factor 1/2 in Eqs. (3) accounts for the two equivalent interfaces per supercell. The chemical potential  $\mu_{\text{Si}}$  (and  $\mu_{\text{Al}}$ ) does not affect the difference between the formation energies of the type-I and -II interfaces. In our calculations we set the value of  $\mu_{\text{Si}}$  to that of the bulk Si chemical potential.<sup>20</sup>

In Fig. 5 we show the Al/GaAs and Al/2 Si ML/GaAs formation energies, for the relaxed type-I and type-II junctions, as a function of the As chemical potential. The formation energies are displayed within the allowed range of values of  $\mu_{\text{As}}$ , as imposed by the inequality (2). The formation energies decrease (increase) with  $\mu_{\text{As}}$  for the type-I (type-II) junctions, according to Eqs. (3). The values of  $\varepsilon_f^{\text{I}}$  and  $\varepsilon_f^{\text{II}}$  computed at  $\mu_{\text{As}} = \mu_{\text{As}}^{\text{bulk}}$  and  $\mu_{\text{As}} = \mu_{\text{As}}^{\text{bulk}} + \Delta H_f$ , respectively, are also reported in Table I for the relaxed and unrelaxed interfaces. The relaxation lowers the formation energies by roughly the same amount for the type-I and type-II interfaces, i.e., by 0.1 eV for a Si coverage  $\theta = 2$  ML and by 0.2 eV for  $\theta = 0$ .

Figure 5 shows that there is a reversal in the relative stability of type-I and type-II interfaces which occurs within the experimentally accessible range of the As (or Ga) chemical potential. This is true for both coverages,  $\theta = 0$  and 2 ML, and we therefore expect this trend to hold also for intermediate coverages  $0 < \theta < 2$  ML. This result yields thus a possible explanation, consistent with the contentions of Refs. 3

and 5, for the effect of the excess cation and anion fluxes on the interface atomic structure, and hence on the Schottky barrier. Under an excess As flux, i.e., at high  $\mu_{\text{As}}$ , the type-I interface is favored with the cation-anion sequence for the dipole layer, resulting in the large  $p$ -type barriers. At sufficiently high cation flux, instead,  $\mu_{\text{As}}$  is low, and the interface termination with the reversed sequence for the local dipole becomes more stable, producing the small  $p$ -type barriers. This explanation for the establishment of the tunable Al/Si/GaAs Schottky diodes is further supported by the quantitative agreement between the computed and experimental Schottky barriers in Table I.

Recent experiments indicated a higher thermal stability of Al/2 Si ML/GaAs junctions with low  $p$ -type barriers (type II) as compared to those with high  $p$ -type barriers (type I).<sup>4</sup> Although the trend of our  $T = 0$  formation energies in Fig. 5 indicates an increase in the stability of the type-II relative to the type-I interfaces with increasing Si coverage, the lowest energies we find are essentially the same (within our numerical accuracy) for the two types of interfaces. In fact, above 300 °C the temperature dependence of the chemical potentials and of the formation energies is expected to become important. Arsenic is known to desorb from GaAs surfaces in vacuum upon annealed above 300 °C, producing increasingly Ga-rich surfaces.<sup>21</sup> A similar behavior for the Al/Si/GaAs junctions may be responsible for the observed trend after annealing at 450 °C.<sup>4</sup> It should be stressed, however, that formation energies alone may be insufficient to explain the different thermal stability of the two types of junctions as the kinetics of the degradation mechanisms may also be important.

## V. CONCLUSION

We investigated from first principles the structural and electronic properties of the Al/Si/GaAs(100) junctions with Ga-terminated and As-terminated GaAs(100) interfaces. The interfacial atomic relaxation was examined, and explained in terms of covalent versus metallic types of bonds established at the interface. For the Al/2 Si ML/GaAs(100) junctions, we found that in contrast to the trend expected from macroscopic elasticity theory, and at variance with the situation in GaAs/2 Si ML/GaAs(100) heterostructures, the Si-Si interplanar distance is *increased* relative to the spacing in bulk Si. This behavior is due to an Al-induced weakening of the covalent bonding of the interlayer.

We also studied the effect of the Si interlayer on the local density of states, and compared the results to the predictions of empirical band-structure models recently proposed to explain the tunable Al/Si/GaAs Schottky barriers.<sup>14</sup> Our *ab initio* results for the coherently strained Al/2 Si ML/GaAs(100) system show that the macroscopic properties of bulk Si postulated in these models are inappropriate to describe the electronic and atomic structures of the interlayer, and hence the tuning established at low Si coverage (0 to 2 ML).

Local interface dipoles produced by the heterovalent Si interlayer at the As- and Ga-terminated GaAs(100) interfaces were found, instead, to quantitatively account for the Schottky barrier tuning in the coherently strained Al/2 Si ML/GaAs(100) systems. Moreover, based on the energetics of the systems, we showed that the relative stability of

the As- and Ga-terminated junctions changes within the experimentally accessible range of the As and Ga chemical potentials. We showed that this change is consistent with the Schottky barriers observed experimentally, and could explain the role of the excess cation and anion fluxes in the establishment of the relevant interface configurations.

#### ACKNOWLEDGMENTS

It is a pleasure to thank A. Franciosi, F. Beltram, and S. De Franceschi for discussions. This work was supported by the Swiss National Science Foundation under Grant No. 20-47065.96. The computations were performed at the CSCS in Manno.

- 
- <sup>1</sup>J. R. Waldrop and R. W. Grant, *Appl. Phys. Lett.* **50**, 250 (1987).
- <sup>2</sup>K. Koyanagi, S. Kasai, and H. Hasegawa, *Jpn. J. Appl. Phys., Part 1* **32**, 502 (1993).
- <sup>3</sup>M. Cantile, L. Sorba, S. Yildirim, P. Faraci, G. Biasiol, A. Franciosi, T. J. Miller, and M. I. Nathan, *Appl. Phys. Lett.* **64**, 988 (1994); M. Cantile, L. Sorba, P. Faraci, Y. Yildirim, G. Biasiol, G. Bratina, A. Franciosi, T. J. Miller, M. I. Nathan, and L. Tapfer, *J. Vac. Sci. Technol. B* **12**, 2653 (1994).
- <sup>4</sup>L. Sorba, S. Yildirim, M. Lazzarino, A. Franciosi, D. Chiola, and F. Beltram, *Appl. Phys. Lett.* **69**, 1927 (1996).
- <sup>5</sup>C. Berthod, N. Binggeli, and A. Baldereschi, *Europhys. Lett.* **36**, 67 (1996).
- <sup>6</sup>W. E. Pickett, *Comput. Phys. Rep.* **9**, 117 (1989), and references therein.
- <sup>7</sup>N. Troullier and J. L. Martins, *Phys. Rev. B* **43**, 1993 (1991); L. Kleinman and D. M. Bylander, *Phys. Rev. Lett.* **48**, 1425 (1982).
- <sup>8</sup>D. M. Ceperley and B. J. Alder, *Phys. Rev. Lett.* **45**, 566 (1980).
- <sup>9</sup>The corresponding cutoff for the Fourier expansion of the charge density is 80 Ry.
- <sup>10</sup>R. G. Dandrea and C. B. Duke, *J. Vac. Sci. Technol. A* **11**, 848 (1993); *J. Vac. Sci. Technol. B* **11**, 1553 (1993).
- <sup>11</sup>H. J. Monkhorst and J. D. Pack, *Phys. Rev. B* **13**, 5188 (1976).
- <sup>12</sup>S. A. Chambers and V. A. Loebs, *Phys. Rev. B* **47**, 9513 (1993).
- <sup>13</sup>We have investigated the effect of the Ga core states on the structural properties of the Ga-terminated junctions using the nonlinear core correction (NLCC). The NLCC is found to increase the GaAs theoretical lattice parameter from 5.55 to 5.59 Å, and to change the lattice relaxation in the Al/GaAs and Al/2 Si ML/GaAs junctions by at most 1%. With the NLCC, the Si-Ga distance in the Al/2 Si ML/GaAs junction is 3% smaller than in bulk GaAs (4% without NLCC), and the Si-Si distance is equal to 1.36 Å (1.38 Å without NLCC), i.e., 3% larger than the MET prediction (as found without the NLCC).
- <sup>14</sup>Z. Chen, S. N. Mohammad, and H. Morkoç, *Phys. Rev. B* **53**, 3879 (1996). These authors revised the band-structure model by J. C. Costa, T. J. Miller, F. Williamson, and M. I. Nathan, *J. Appl. Phys.* **70**, 2173 (1991), to incorporate the effect of strain on the Si band gap.
- <sup>15</sup>R. People, *Phys. Rev. B* **34**, 2508 (1986).
- <sup>16</sup>G.-X. Qian, R. M. Martin, and D. J. Chadi, *Phys. Rev. B* **38**, 7649 (1988).
- <sup>17</sup>P. Eckerlin and H. Kandler, in *Structure Data of Elements and Intermetallic Phases*, Landolt-Börnstein, New Series, Group III, Pt. 6 (Springer-Verlag, Berlin, 1971), p. 1.
- <sup>18</sup>The calculations for the As (Ga) metallic phase were performed with 116 (75) inequivalent  $k$  points in the Brillouin zone. With our choice of  $k$  points grids, the densities of points in reciprocal space were similar for the As and Ga phases.
- <sup>19</sup>M. Tmar, A. Gabriel, C. Chatillon, and I. Ansara, *J. Cryst. Growth* **69**, 421 (1984).
- <sup>20</sup>We calculated  $\mu_{\text{Si}}$  at the theoretical lattice parameter of Si 5.39 Å (exp. 5.43). Our formation energies for Al/Si/GaAs include therefore also the strain energy of the Si interlayer.
- <sup>21</sup>W. Chen, M. Dumas, D. Mao, and A. Kahn, *J. Vac. Sci. Technol. B* **10**, 1886 (1992); D. K. Biegelsen, R. D. Bringans, J. E. Northrup, and L.-E. Swartz, *Phys. Rev. B* **41**, 5701 (1990).